MICROPOROSITY AND ITS EFFECT ON THE FATIGUE BEHAVIOR OF 7050-T7451 THICK PLATE

X. Xiao, H.X. Jiang and CH. Liu

Chinalco Materials Application Research Institute Beijing 102209, China
(*Corresponding author: xiaoxiang_zhl@163.com*)

ABSTRACT

A study has been conducted to characterize the fatigue life in 7050-T7451 thick plate by the comparison between an experimental alloy and commercial alloy. The fracture origins were specified and their sizes were measured by scanning electron microscope (SEM). Additionally, the size, number density and spatial distribution of porosity in the experimental material and commercial material were characterized and compared, using X-ray Computed Tomography (XCT). The results showed that microporosity was the predominant site for crack nucleation and subsequent failure of the experimental alloy. However, as for the commercial alloy, fatigue cracks were found to originate from constituent particles. The presence of microporosity in 7050-T7451 thick plate reduced fatigue life of an order of magnitude or more compared to the commercial alloy. The relationships between size of origin and fatigue life were proposed. It was showed that the fatigue endurance was reduced when the size of porosity increased.

KEYWORDS

Microporosity, fatigue life, X-ray Computed Tomography, 7050 thick plate

INTRODUCTION

7xxx series aluminum alloys, due to their combination of high strength, high resistance to stress corrosion cracking, and good fracture toughness, are widely used in structural engineering applications where high-strength and low-density characteristics are fundamental design requirements (Williams & Starke, 2003). Every designer is striving to find an optimal combination of properties including strength, corrosion resistance and fatigue resistance (Wang et al., 2016). Based on the design principles of aircraft, a higher fatigue resistance of aluminum alloys are required. Thus, many investigations have been carried out on the microstructures and its effect on fatigue properties of the 7xxx series aluminum alloy (Robson, 2004; Schubbe, 2009).

Microporosity, which is a common defect in casting materials, can lead to a significant deterioration of mechanical performance and fatigue resistance, especially in the high alloyed 7xxx aluminum alloys. The actual valid loading area decreases due to microporosity, which results in detrimental effect on the mechanical properties. Many experimental studies have been conducted in this research field. Mayer et al. (2003) investigated the fatigue properties of magnesium alloys produced by high-pressure die-casting. The results show that porosity in magnesium alloys greater than 0.18 mm diameter may be considered as the most important material defect for high cycle fatigue and fully reversed loading conditions. Nadot et al. (2004) found that the near surface defects are much more dangerous than the internal defects. Wang et al. (2001a) used the Weibull statistics method to analysis the influence of the microporosity, oxides and particles on the A356-T6 alloy fatigue life. The results show that, the porosity is more detrimental to fatigue life than oxide films and particles. With regard to fatigue resistance, although the deleterious effect of microporosity has been generally acknowledged, a quantitative understanding between casting microporosity and fatigue life in 7050-T7451 plate is not well established.

To achieve this end, we have made extensive use of X-ray Computed Tomography (XCT) to quantify the size, morphology, frequency, and distribution, in three dimensional spaces, of the porosity found in test samples. This has allowed statistically valid results to be obtained with far more detailed information. By using XCT systems with different resolutions, it has been possible to quantify the position of the full size range of porosity to the beam scanning strategies, as well as to measure the true sizes and morphologies of the porosity (Kuwazuru et al., 2008; Buffiere et al., 2001).

In this contribution fatigue tests were conducted on the experimental and commercial materials. The defects observed on the fatigue fracture surfaces after the fatigue text were compared. The relationships between size of origin and fatigue life were proposed. These results can make a great help for understanding the mechanism and rules of micro-porosity's effects on fatigue resistance of 7050-T7451 thick plate alloy, including porosity's morphology, distribution, and size and so on.

MATERIALS AND EXPERIMENTAL METHODS

Materials

The raw materials used in the present study are commercially available and experimental 7050-T7451 thick plate (150 mm thickness). The morphology of the constituent phase is examined on JSM-5600 scanning electron microscopy (SEM). The second phase particles are identified by energy dispersive X-ray spectrometry (EDX).

X-Ray CT Inspection

The testing system for XCT inspection is a visualization apparatus equipped material testing system: Y.CT PRECISION S. The X-ray tube voltage can reach 225 kV. The resolution of CT image used is 1024×1024 pixels and the slice pitch is about 30 μm.

Fatigue Test

The fatigue test (stress ratio R=0.1) is carried out at room temperature with a sinusoidal signal of 30Hz at 241MPa stress in ambient air by the servo-hydraulic fatigue testing machines. Test pieces are taken from the 1/2 thickness locations of the plate and machined into the shape in accordance with AMS-4050H standard, as shown in Figure 1. For thick plate, the microporosity is more severe at the center of the thickness of the ingot. After the fatigue tests, crack initiation sites are specified and their sizes are measured by scanning electron microscope (SEM). In addition, the run-out test pieces are broken by cyclic overloading with higher stress of 341 MPa than that used in fatigue tests.
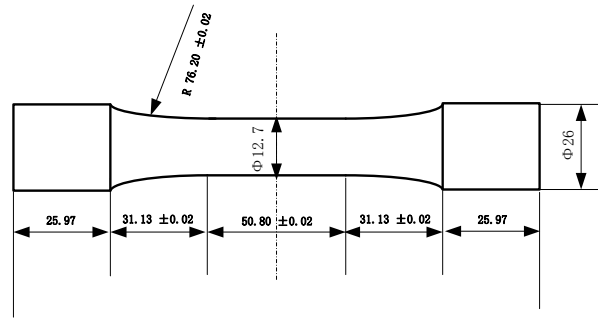
Figure 1. Fatigue test piece

Microporosity Measurement

The microporosity of the test specimens are measured by quantitative fractography of surfaces fractured during the fatigue tests. These quantitative fractographic analyses involve the examination of SEM images of the fractured test specimen surfaces. The value of the $(area)^{1/2}$ is used as characterizing porosity size and as severity indicator in fatigue.

RESULTS

Microstructure

Typical examples of the microstructure of experimental and commercial alloy specimens are shown in Figure 2. There are undissolved coarse phase in all two kinds of plates. The coarse second phase particles shown as white are presented as clusters of fragmented along the rolling direction. The microstructure consists of S and Fe-rich phases. The S particles have a rounded shape on the metallographic section.
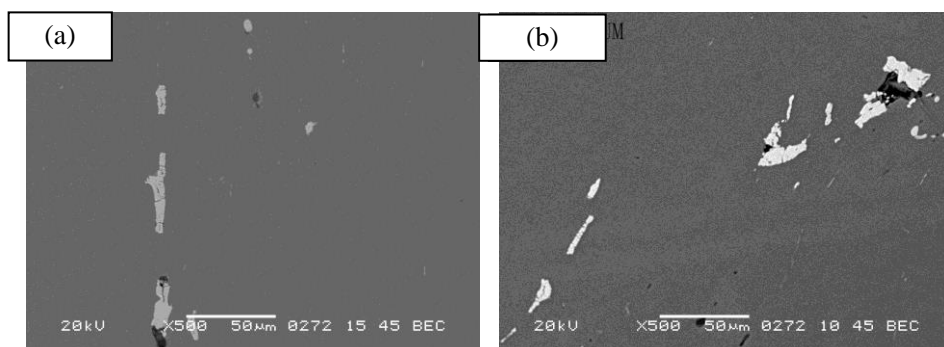
Figure 2. The microstructure of experimental (a) and commercial (b) alloy in SEM image

Fatigue Life and Fractographic Examination

Table 1 shows the low cycle fatigue life of experimental and commercial alloy. Results show that the fatigue life of all experimental alloy samples is lower than 15×10^4 cycles, which does not meet the AMS-4050H standard. It is worth noting that the fatigue life of commercial alloy exceeds 20×10^4 cycles.

Table 1. Fatigue life and characteristics of fatigue sources of experimental and commercial alloy

Material	Specimen	Fatigue life (cycles)	Fatigue crack origins	Size (µm)	
				Equivalent radius	Depth in the fatigue crack propagation direction
Experimental	1	80,987	porosity	60	146
	2	84,720	porosity	58	303
	3	65,741	porosity	79	332
	5	47,907	porosity	104	255
	6	60,102	porosity	77	236
	7	111,840	porosity	59	50
	8	81,708	porosity	33	70
	10	50,299	porosity	75	526
	11	56,984	porosity	95	216
	12	77,383	porosity	38	151
	13	76,000	porosity and particles	28	482
Commercial	14	>200,000	particles	20	

The typical fracture surfaces of both the experimental and commercial alloy are shown in Figure 3 and Figure 4. It shows the photograph and schematics of the fracture surface. The crack initiates at the surface on the machined surface as observed in the normal fatigue tests.
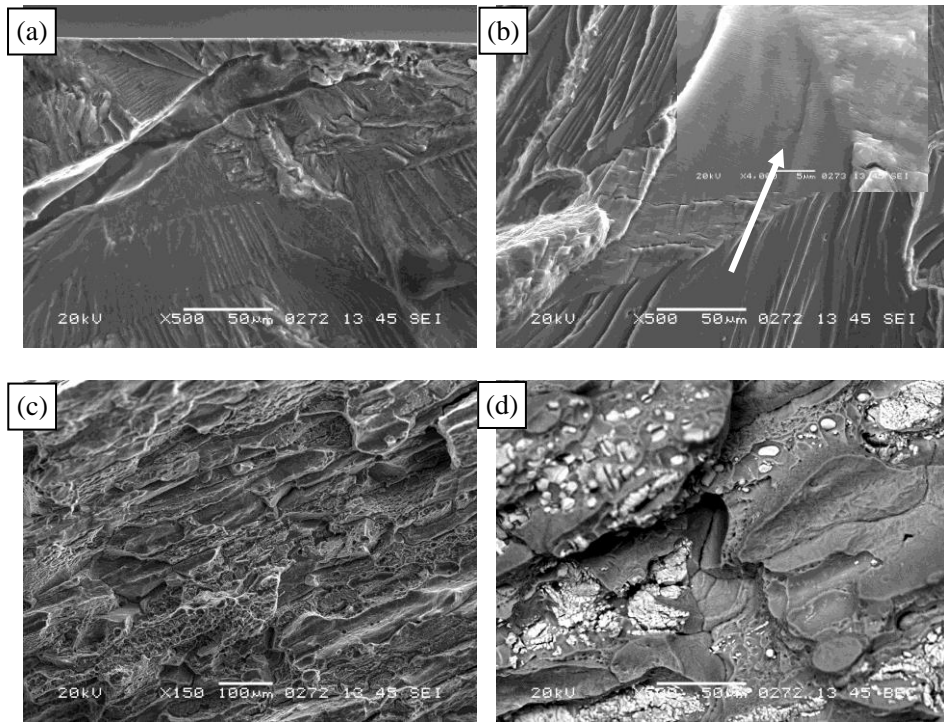
Figure 3. Fracture surfaces of experimental material: (a) fatigue crack origin, (b) fatigue crack propagation, (c) fracture zone and (d) corresponding back scattered-electron image
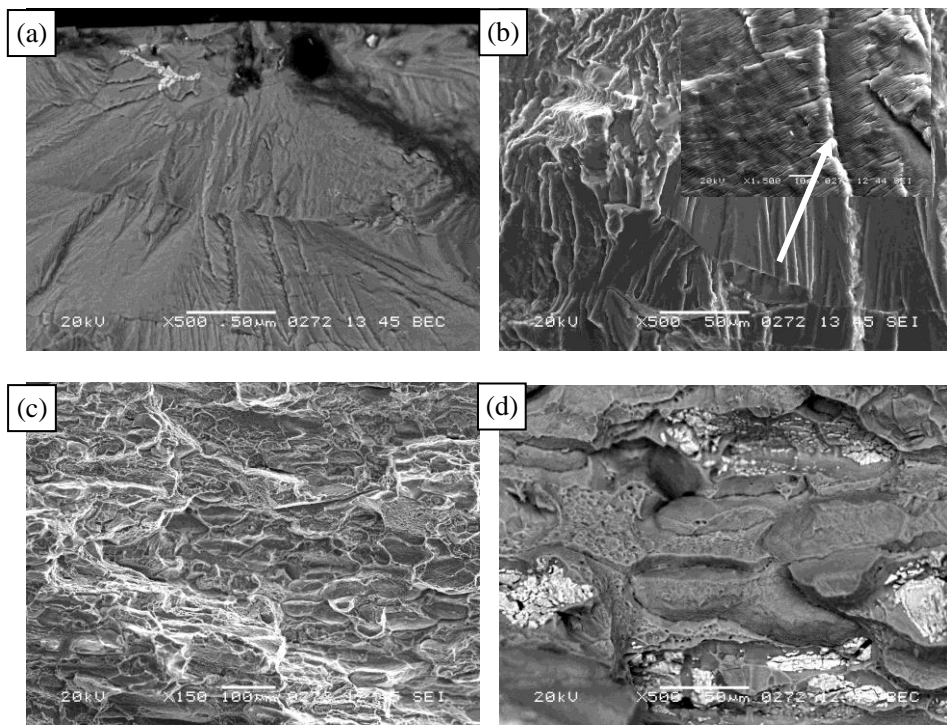
Figure 4. Fracture surfaces of commercial material: (a) fatigue crack origin, (b) fatigue crack propagation, (c) fracture zone and (d) corresponding back scattered-electron image

Results show that the fatigue crack origin between the experimental and commercial alloy is different. For the experimental alloy, the fatigue fracture occur because of the presence of microporosity on or near the free surface of the specimen. As for the commercial alloy, the fatigue crack origin is the coarse particles (Fe-rich phase and S phase). The statistics characteristics of fatigue sources at different samples are shown in Table 1.

Some selected fatigue specimens during the fatigue tests of experimental material were examined in SEM. Figure 5 shows typical appearances of the fracture crack origins in different specimens. It is shown that the fatigue cracks originate from microporosity. The porosity size is determined directly from the SEM pictures by measurements of the porosity area. The equivalent radius are calculated by assuming a circular defect area in the cross section. It is worth noting that the size and location of microporosity in fatigue crack origin of each samples are different as shown in Table 1. The equivalent radius of the critical defect at the fatigue crack origins of the specimens, have the size region 28–104 μm. All materials have wide distribution in fatigue life. The variations can be caused by the ones of size of microporosity at the origins.

In the steady propagated area seen in Figure 3(b) and Figure 4(b), typical fatigue striations, fatigue steps, dimples, and secondary cracks can be observed. Figure 3(c) and Figure 4(c) reveal that the final fracture regions are mainly consisted of intergranular fracture and transgranular dimples, which are similar to characteristic of tensile fracture. Fractographic examination of the broken specimens reveal that most of the fracture surfaces are mostly covered by striations. Nevertheless, in some zones the presence of coarse particles (Fe-rich phase and S phase) are observed in both alloys, as shown in Figure 3(d) and Figure 4(d). These particles accelerate the failure process. The decohesion between the particles and the surrounding matrix generates microvoids that facilitate the crack propagation.
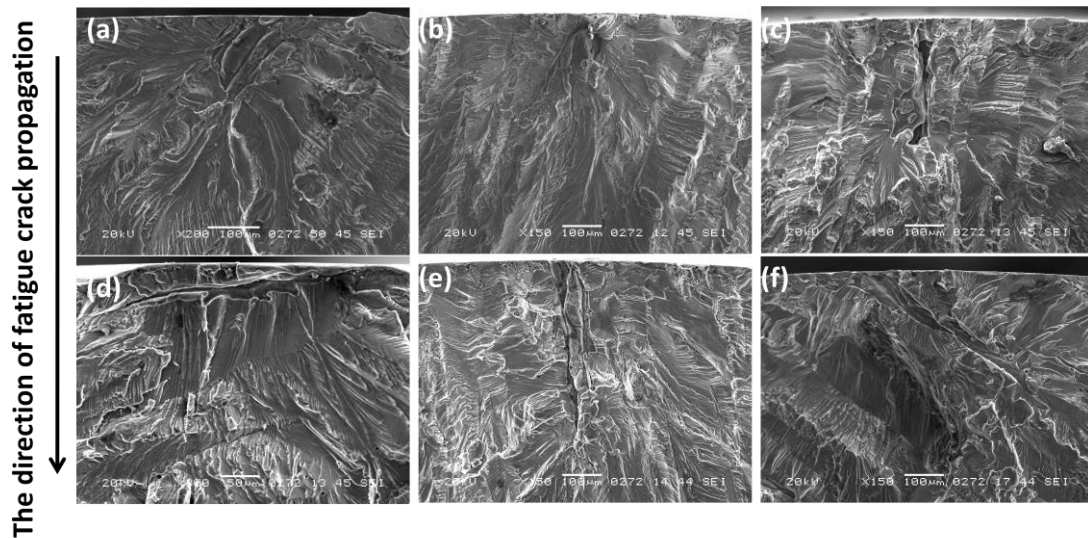
Figure 5. The fatigue crack origins of different samples: (a) Sample 1, (b) Sample 2, (c) Sample 3, (d) Sample 8, (e) Sample 10, (f) Sample 11

XCT Quantifications

Figure 6 shows the XCT results of the experimental and commercial 7050 plates. And the color area in the map shows a defect. The results show that there exists many micro porosities in the plates. Table 2 shows the statistics results of the number density and average equivalent diameter of the porosity in the two alloys. It can be found that the experimental alloy has more defects, and the number density of the porosity is higher than that of the commercial one. The average equivalent diameter of the porosity in

experimental alloy is less than that of commercial one.

Table 2. Statistical results of the porosity in the two alloys

Alloy	Commercial alloy	Experimental alloy
Porosity, %	0.001	0.008
Number density, mm^{-3}	0.33	0.468
Euqivalent diameter, μm	41	60
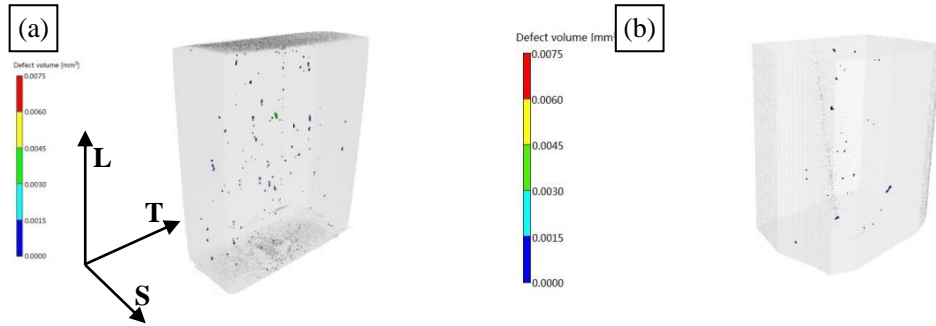
Figure 6. XCT results of the experimental (a) and commercial (b) 7050 plates

Figure 7 shows the typical image of microporosity in the L-S direction of experimental alloy. The coordinate X in the graph represents the direction of the thickness S, Y represents the T direction, Z represents the rolling L direction. It shows that, after hot rolling, the microporosity tending to elongate along the rolling direction. The distribution frequency and cumulative frequency of microporosity in different sizes of the experimental alloy and commercial alloy are shown in Figure 8. Figure 9 shows the size distribution of microporosity in both alloys. It can be seen that when the cumulative frequency is 90%, the equivalent diameter of porosity in experimental alloy and commercial alloy is respectively as 97 μm and 58 μm. The maximum equivalent diameter of the porosity in the commercial alloy is less than 60 μm, while the largest porosity in the experimental alloy reaches 200 μm. It seems that the numbers density of microporosity in the experimental alloy is apprently more than that of the commercial alloy, which is accordance with the fractographic examination results.
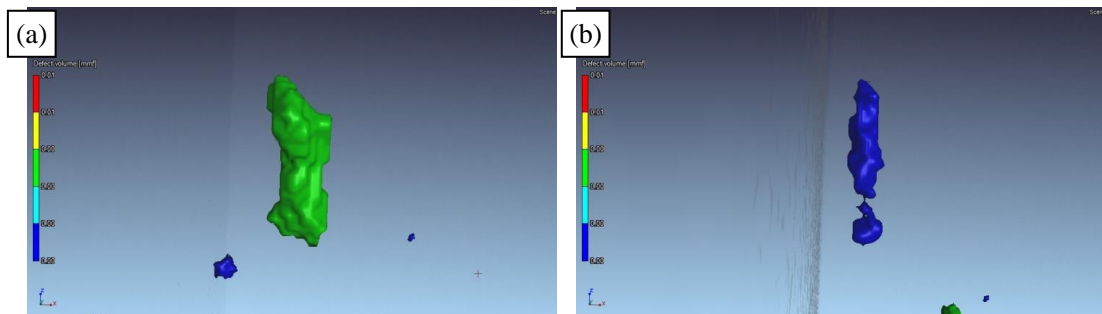
Figure 7. Typical XCT images of microporosity in experimental alloy
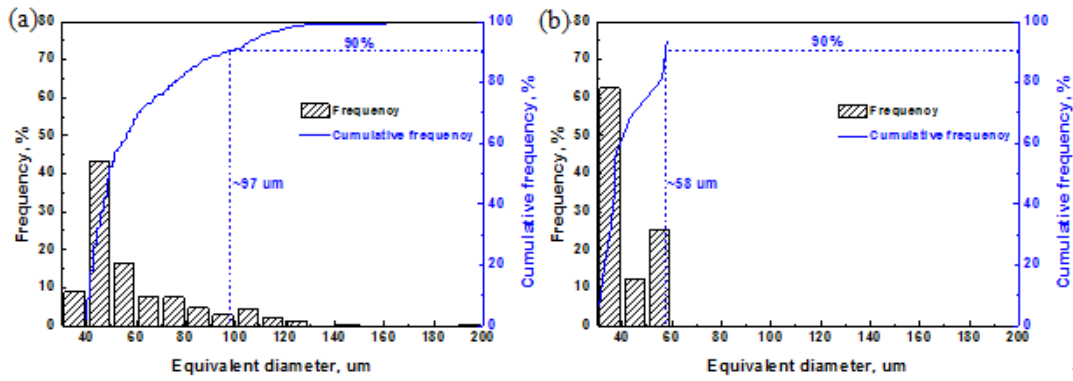
Figure 8. The distribution frequency and cumulative frequency of microporosity in different size range of the experimental alloy (a) and commercial alloy(b)
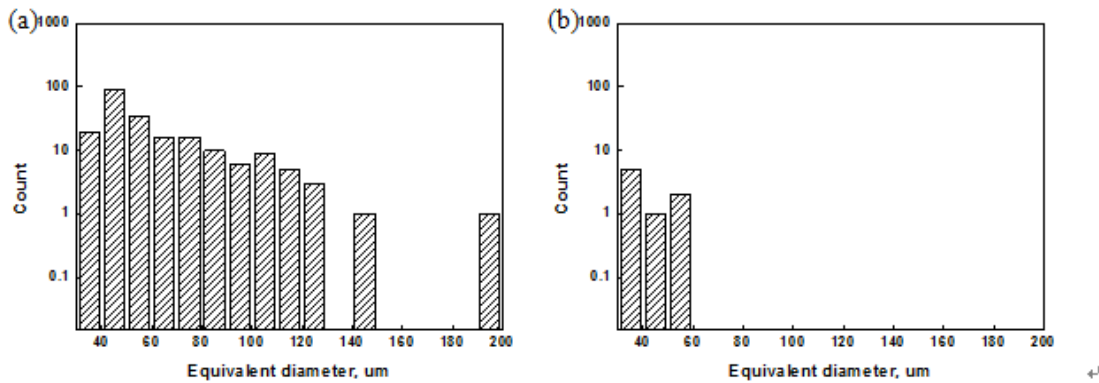
Figure 9. The size distribution of the experimental alloy (a) and commercial alloy (b)

DISCUSSION

Fatigue life N_f consists of fatigue crack initiation life N_i and fatigue crack propagation life N_p. Among them, N_i includes crack initiation stage and growth stage (the first stage). N_p contains macro-crack expansion stage (second stage expansion) and final failure period, while there are only several cycles in the transient period. Generally speaking, the crack forming life N_i occupies a large proportion in the total life N_f, even up to 80% of the total life.

It is claimed that the fatigue crack is initiated at the largest defect and grows up to final failure surface (Wang et al., 2001; Zhang et al., 2000). The maximum defects are statistically evaluated on the basis of the fracture surface inspection in this paper. For the experimental alloy samples as shown in Figure 5, the microporosity is the largest microstructure defect present. The size of microporosity is considerably larger than the particles (20 μm), seen in Table 1. Fatigue cracks are found to originate from porosity rather than from particles. In Figure 10, the fracture-initiating porosity size is plotted as a function of the number of cycles to failure for the experimental alloy. It seems that the longest fatigue life is expected for the specimens with the smallest pores. As for the sample 5, the fatigue life is lowest, and the equivalent radius of microporosity is largest 104 μm. The number of cycles to the fatigue fracture is assumed to increase with the porosity size decreasing.
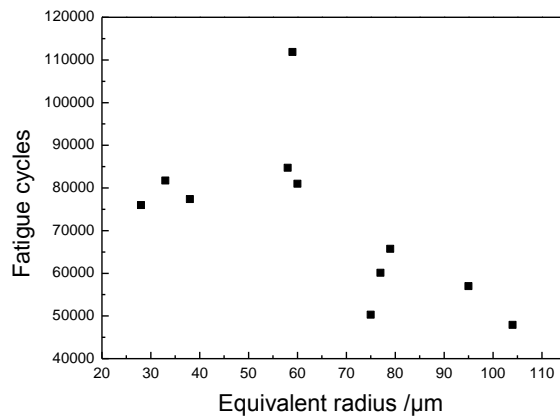
Figure 10. Relationship between the fracture-initiating porosity size and the fatigue life

The fatigue life correlates rather well with the measured initiating porosity size. The examination of the fracture surface shows that the microporosity is the important microstructural feature for the fatigue failure under the present conditions. The number of cycles to failure for a given stress level can be correlated to the size of the porous area at the crack initiation place, i.e. the larger the defect area the lower the fatigue lifetime, which is similarly to cast aluminium (Wang, 2001; Zhang et al., 2000).

The large distributed microporosity in the microscale finally leads to the degeneration of fatigue resistance in the macroview. In the region of microporosity, stress concentration can be formed, since local large-section change exists and the actual bearing area decreases. From the X-ray CT inspections, we found that the shrinkage cavities have a complicated surface shape consisting of the exposed dendrites, while the shape of gas pores are smooth and spherical in general. Consequently, the stress concentration becomes higher by the locally large curvature of shrinkage cavities than by the small curvature of gas pores.

The presence of microporosity in this alloy reduces fatigue life of an order-of magnitude or more compared to a defect-free material because practically eliminates the crack initiation phase. It is also found that there is a threshold defect size for fatigue crack initiation from a pore (Fintova et al., 2010). According to Table 1, the smallest equivalent radius of microporosity in the fatigue crack origins of the experimental alloy is about 28 μm. From the X-ray CT results seen in Table 2, the average equivalent diameter of the porosity in the experimental and commercial alloy is respectively as about 41 μm and 60 μm. It can be speculated that the critical size of the porosity (in equivalent radius) is about 20–30 μm. Below this threshold size, fatigue crack initiation occurs at Fe-rich phase and S phase eutectic particles, as showen in Figure 4.

Lifetimes measured for materials containing porosity are typically subjected to increased scatter, since the cyclic properties of specimens depend on the sizes of eventual porosity and their location in the stressed volume, i.e. in the interior or at the surface. When the number of microporosity is few, the size is small, and locates in the steady propagated area and final fracture region, the porosity has no influence in the fatigue performance of materials. The crack initiation source is not always the maximum porosity in the specimen, and is basically restricted to porosity near the outer surface.

The direction of microporosity also affects fatigue life, as shown in Figure 5. For specimens 1, 2 and 7 with the same equivalent radius of porosity about 60 μm, the size of porosity in the direction of the fatigue crack growth differ considerably among each other, respectively as 146 μm, 303 μm and 50 μm. The fatigue cycle times of the specimen 7 with the less depth (50 μm) are longer (111,840 cycles). While in sample 1 the fatigue cycle times of greater depth (146 μm) are shorter (80,987 cycles). The XCT results

show that the length of the microporosity in the rolling direction is equivalently large, since the porosity is easy to stretch in the process of hot rolling. It is known that the length of the microporosity in the fatigue crack growth direction is equivalent to the initial crack length. With the length of the crack increases, the loading time of the initiation crack process into the fatigue growth stage became more quickly. When the direction of the maximum diameter of microporosity coincidence with the fatigue growth direction, the fatigue life is shorter.

Microporosity is the most typical defects, which is induced by entrapped or discharged gases and sometimes expanded by shrinkage of solidified material. The porosity size and shape are highly dependent on the casting process, that is, the molten material flow and solidification process. From the statistics results, the fatigue crack origin of the experimental alloy is microporosity. Moreover, the size and the direction of the porosity influence the fatigue life. Therefore, the fatigue property of the plate is strictly related to the porosity control.

CONCLUSIONS

The following conclusions can be drawn from this study:
(1) Microporosity defects have a detrimental effect on fatigue life by shortening fatigue crack initiation period. The equivalent size of the microporosity is the key factor controlling fatigue lifetime in 7050 aluminum alloys. The size, location and direction of microporosity causes great variability in fatigue lifetime. Plates with microporosity show at least an order of magnitude lower fatigue life compared to defect-free materials.
(2) There exists a critical defect size for fatigue crack initiation, below which the fatigue crack initiates from other instrinsic initiators such as Fe-rich phase and S phase. In 7050-T7451 alloy, the critical defect size (equivalent radius) is in the range of about 20–30 μm.

REFERENCES

Buffiere, J. Y., Savelli, S., Jouneau, P. H., Maire, E., & Fougeres, R. (2001). Experimental study of porosity and its relation to fatigue mechanisms of model Al−Si7−Mg0.3 cast Al alloys. *Materials Science and Engineering A, 316, 115−126.*

Fintova, S., Konecna, R., Nicoletto, G. (2010). Influence of shrinkage porosity on the fatigue behavior of cast AlSi7Mg. *Roznov pod Radhostem, Czech Republic, EU.*

Kuwazuru, O., Murata, Y., Hangai, Y., Utsunomiya, T., Kitahara, S., & Yoshikawa, N. (2008). X-Ray CT Inspection for Porosities and Its Effect on Fatigue of Die Cast Aluminium Alloy. *Journal of Solid Mechanics and Materials Engineering, 2, 1220-1231.*

Mayer, H., Papakyriacou, M., Zettl, B., & Stanzl-Tschegg, S. E. (2003). Influence of porosity on the fatigue limit of die cast magnesium and aluminium alloys. *International Journal of Fatigue, 25, 245-256.*

Nadot, Y., Mendez, J., Ranganathan, N. (2004). Influence of casting defects on the fatigue limit of nodular cast iron. *International Journal of Fatigue, 26, 311-319.*

Robson, J. D. (2004). Microstructural evolution in aluminium alloy 7050 during processing. *Materials Science and Engineering A, 382, 112-121.*

Schubbe, J. J. (2009). Fatigue crack propagation in 7050-T7451 plate alloy. *Engineering Fracture Mechanics, 76, 1037-1048.*

Wang, J. S., Kang, Y. W., & Li, Ch. R. (2016). Phase Diagram and Phase Equilibrium Studies on Ultra High Temperature Alloys of Nb-Si-Ti. *Materials Science Forum, 849, 618-625.*

Wang, Q. G., Apelian, D., & Lados, D. A. (2001a). Fatigue behavior of A356-T6 aluminum cast alloys. Part I. Effect of casting defects. *Journal of Light Metals, 1, 73-84.*

Wang, Q. G., Apelian, D., & Lados, D. A. (2001b). Fatigue behavior of A356/357 aluminum cast alloys. Part II. Effect of microstructural constituents. *Journal of Light Metals, 1, 85-97.*

Williams, J. C., & Starke E. A. (2003). Progress in structural materials for aerospace systems. *Acta Materiali, 51, 5775-5799.*

Zhang, B., Chen, W. & Poirier, D. R. (2000). Effect of solidification cooling rate on the fatigue life of A356.2-T6 cast aluminium alloy. *Fatigue Fract Engng Mater Struct, 23, 417-423.*